

# The non-polar solvent potential of mean force for the dimerization of alanine dipeptide: the role of solute–solvent van der Waals interactions

Yang Su, Emilio Gallicchio\*

*Department of Chemistry and Chemical Biology, BIOMAPS Institute, Rutgers University, Wright-Rieman Laboratories, 610 Taylor Rd, Piscataway, NJ 08854-8087, USA*

Received 9 October 2003; received in revised form 9 October 2003; accepted 20 November 2003

---

## Abstract

The non-polar component of the potential of mean force of dimerization of alanine dipeptide has been calculated in explicit solvent by free energy perturbation. We observe that the calculated PMF is inconsistent with a non-polar hydration free energy model based solely on the solute surface area. The non-linear behavior of the solute–solvent van der Waals energy is primarily responsible for the non-linear dependence of the potential of mean force with respect to the surface area. The calculated potential of mean force is reproduced by an implicit solvent model based on a solvent continuum model for the solute–solvent van der Waals interaction energy and the surface area for the work of forming the solute cavity.

© 2003 Elsevier B.V. All rights reserved.

*Keywords:* Potential of mean force; Implicit solvent model; Alanine dipeptide; Non-polar solvation; hydrophobicity; Free energy perturbation; Dimerization

---

## 1. Introduction

Biochemical processes take place in water and it is important to consider solvent effects on their thermodynamics. Computer simulations are increasingly being employed to understand and predict properties of biological systems at the atomic level. Hydration free energy models are nowadays widely used to account for solvent effects in computer models for protein structure prediction, protein folding, and binding [1–3].

\*Corresponding author. Tel.: +1-73-2445-5157; fax: +1-73-2445-5958.

*E-mail address:* emilio@hpcp.rutgers.edu (E. Gallicchio).

Explicit solvent models [4] provide the most accurate and complete description of hydration phenomena but they are computationally very demanding. The potential of mean force (PMF), defined as the hydration free energy of each conformation of the solute [5], is in principle obtainable with arbitrary accuracy from explicit solvent hydration free energy perturbation (FEP) calculations. Implicit solvent models, provide approximations to the PMF, and make it possible to obtain thermodynamics properties of the solute without having to explicitly follow the solvent degrees of freedom.

Implicit solvent models based on continuum dielectric (polar hydration) and surface area (non-polar hydration) models are widely used [5–9]. Studies have been carried out in this laboratory to test continuum dielectric models against explicit solvent FEP calculations [10,11] and experiments [12,13]. Empirical surface area models are based on a linear relationship between the solvent accessible surface area and the non-polar hydration free energy [6]. Although surface area models have served as a useful first approximation, deficiencies have been reported [7]. Furthermore, there is growing evidence that the surface tension parameters of surface area models are not readily transferable between different systems [7,6,11]. Several studies have attributed the deficiencies of surface area models to their inability to fully capture the properties of the solute–solvent dispersion interactions [11,14–16]. Due to the medium range nature of dispersion interactions, the solute–water van der Waals interaction energy due to atoms not directly exposed to the solvent is substantial [11,16], and a large degree of variation of van der Waals interaction energies are observed for solute atoms with similar solvent accessible surface areas [11]. These phenomena contribute to the limited accuracy of linear surface models for high resolution modeling studies of protein folding and binding [11].

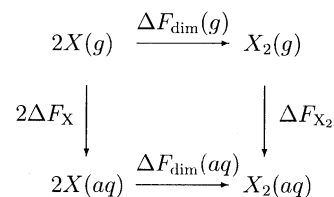
Gallicchio et al. [14] rationalized the smaller than expected hydration free energies of cyclic alkanes by showing that the free energy change to establish the solute–solvent dispersion interactions of small alkanes depends mainly on their atomic composition rather than on their surface area [14,17,18]. Surface area models have also been notoriously inadequate in describing the PMF of dimerization of hydrophobic monoatomic solutes in water. The general view of hydrophobic interactions is based on the assumption that hydrophobicity drives non-polar molecules together. The driving force for hydrophobic aggregation is consistent with the solvent trying to minimize the surface area of the solute–solvent interface [19,20]. The PMF of dimerization of hydrophobic monoatomic solutes in water obtained from computer simulations and analytical theories [15] [21–26] show, however, a free energy barrier between

the contact state and the solvent-separated state [23], which cannot be reproduced by the surface area models. Pitarch et al. [15] reported that the van der Waals interaction energy between a methane dimer and water is nearly independent of the dimer solvent accessible surface area. However, it was shown that a surface area model is consistent with the calculated free energy of association of plate-like molecules, which lack attractive dispersion interactions with the water solvent [20]. These observations indicate that the deficiencies of surface area models for modeling the thermodynamics of hydrophobic aggregation are related to the inability of surface area models to fully capture the properties of solute–solvent dispersion interactions.

In this study, we investigate in detail the role of solute–solvent dispersion forces in the hydrophobic aggregation of simple molecules of biological interest. We calculate the non-polar component of the PMF of dimerization of alanine dipeptide by means of the free energy perturbation (FEP) method and molecular dynamics (MD) sampling in explicit solvent. The study of the dimerization of alanine dipeptide is a useful paradigm in the understanding of the physics of  $\beta$ -hairpin and  $\beta$ -strand formation in proteins. We show that a model [13,27] based on the cavity and solute–solvent dispersion energy decomposition of the non-polar hydration free energy successfully reproduces the calculated PMF of dimerization. This work further motivates the use, in the context of implicit solvent models, of a non-polar free energy model based, in addition to the the solute surface area, also on geometrical estimators better suited to describe solute–solvent dispersion interactions.

## 2. Theory and methods

The thermodynamic cycle used to calculate the solvent potential of mean force of dimerization [21] is:



where  $X$  represents the monomer and  $X_2$  represents the dimer.  $\Delta F_X$  and  $\Delta F_{X_2}$  represent the solvation free energies of the monomer and the dimer, respectively.  $\Delta F_{\text{dim}}(g)$  and  $\Delta F_{\text{dim}}(aq)$  represent the dimerization free energies in gas phase and the aqueous phase, respectively.

The solvation contribution to the free energy of dimerization is:

$$\Delta\Delta F = \Delta F_{\text{dim}}(aq) - \Delta F_{\text{dim}}(g) = \Delta F_{X_2} - 2\Delta F_X \quad (1)$$

We model each monomer as a rigid molecule. In this case, it can be shown that  $\Delta\Delta F$  is given by the free energy of dimerization in solution neglecting the intramolecular and monomer–monomer interactions; that is by considering only solute–solvent interactions.

In order to calculate the non-polar hydration free energy contribution to the free energy of dimerization, we calculate the free energy of dimerization between two uncharged alanine dipeptide molecules.

### 2.1. Explicit solvent free energy perturbation calculations

The solvent potential of mean force is determined as a function of the separation distance ( $d$ ) between the  $C_\alpha$  atoms of the two alanine dipeptide monomers. We employ the FEP method in explicit solvent with MD sampling.

We perform MD simulations with the distance  $d$  constrained at the value  $d_i$  and calculate the reversible work for changing the separation distance by  $\delta d$  using the FEP formula:

$$\begin{aligned} \Delta F_{i+1,i} &= F(d_i + \delta d) - F(d_i) \\ &= -kT \ln \langle \exp(-\beta[U(d_i + \delta d) \\ &\quad - U(d_i)]) \rangle_i \end{aligned} \quad (2)$$

where  $U(d_i)$  is the instantaneous solute–solvent potential energy of state  $i$  and  $U(d_i + \delta d) - U(d_i)$  is the variation of potential energy due to changing the dimerization distance from  $d_i$  to  $d_i + \delta d$ ,  $\langle \dots \rangle_i$  indicates an ensemble average in state  $i$ . In our

implementation, state  $i=0$  corresponds to the two monomers separated by the largest distance and the state  $i=N$  corresponds to the dimer. The free energy of dimerization is obtained by summing over the intermediate states:

$$\begin{aligned} \Delta\Delta F &= -kT \sum_{i=0}^{N-1} \ln \langle \exp(-\beta \\ &\quad \times [U(d_i + \delta d) - U(d_i)]) \rangle_i \end{aligned} \quad (3)$$

The dimer structure is prepared in the beta–sheet parallel conformation, the distance,  $d$ , between the two  $C_\alpha$  atoms is 6.3 Å. One monomer is gradually moved away from the other in the plane of the beta–sheet by controlling the distance  $d$  between the two  $C_\alpha$  atoms. The largest separation distance between the monomers is 14.5 Å.

We divide the dimerization transformation into 160 steps by varying the intermolecular distance in steps of  $\delta d = 0.0565$  Å. We carry out two separated FEP simulations, one starting from the dimer state, and the other in the reverse direction. The difference between the two energy profiles is a measure of the systematic error due to the hysteresis.

The simulation is prepared by placing the uncharged dimer at the center of a box of dimensions  $27.92 \times 27.92 \times 27.92$  Å with 688 TIP4P [28] water molecules. The water molecules, which overlap with the solute molecules are removed. Periodic boundary conditions are applied. The cutoff for the non-bonded interactions is 13.5 Å. FEP/MD simulations are carried out at constant temperature and constant pressure at 298.15 K and 1 atm. All the simulation are carried out using the IMPACT software package [29]. The SHAKE algorithm is used to constrain the bond lengths and bond angles of the solvent molecules. At each FEP step, the system is equilibrated for 10 ps. Collection time is 16.8 ps at each FEP step.

### 2.2. Solute–solvent dispersion energy component of the free energy of dimerization

The non-polar solvation process is considered as divided into two steps. First, a cavity with the

same shape as the solute molecule is created in solvent, then, the attractive van der Waals interactions between the solute molecule and the solvent are added. The solute cavity solvation free energy corresponds to the work of growing the repulsive component,  $u_{\text{rep}}(r)$ , of the solute–solvent interaction potential. The free energy of adding the attractive van der Waals interaction corresponds to the attractive van der Waals solute–solvent interaction  $u_{\text{vdw}}(r)$ .

The solute–solvent site–site dispersion interaction energy is modeled using the standard 12–6 Lennard–Jones pair potential,  $u_{\text{LJ}}$ . The Lennard–Jones pair potential energy is decomposed into repulsive and attractive components using the Weeks–Chandler–Andersen (WCA) decomposition scheme [30] as follows:

$$u_{\text{LJ}}(r) = u_{\text{rep}}(r) + u_{\text{vdw}}(r) \quad (4)$$

where

$$u_{\text{rep}}(r) = \begin{cases} u_{\text{LJ}}(r) + \varepsilon & r \leq 2^{1/6}\sigma \\ 0 & r > 2^{1/6}\sigma \end{cases} \quad (5)$$

$$u_{\text{vdw}}(r) = \begin{cases} -\varepsilon & r \leq 2^{1/6}\sigma \\ u_{\text{LJ}}(r) & r > 2^{1/6}\sigma \end{cases} \quad (6)$$

where  $\sigma$  and  $\varepsilon$  are the radius and well-depth parameters of the Lennard–Jones potential,  $u_{\text{rep}}(r)$  is the short-range repulsive component of the standard LJ potential, and  $u_{\text{vdw}}(r)$  is the attractive components of the Lennard–Jones potential.

Studies of alkane hydration with the WCA decomposition of the Lennard–Jones potential showed that the free energy of cavity formation,  $\Delta F_{\text{cav}}$ , is uncorrelated with the free energy change corresponding to adding the van der Waals interactions,  $\Delta F_{\text{vdw}}$  [14]. The former was found to be linearly correlated with the solvent accessible surface area, whereas  $\Delta F_{\text{vdw}}$  was found in some cases to be independent of the surface area. Studies on proteins and protein complexes yielded similar conclusions [11].

It has also been found that the entropic and solvent reorganization energy components of

$\Delta F_{\text{vdw}}$  are negligibly small. Calculations in water show that  $\Delta F_{\text{vdw}}$  is, within 2% accuracy, equal to the average of the WCA attractive component,  $U_{\text{vdw}}$ , of the solute–solvent interactions energy [14]. Thus, we approximate the free energy change  $\Delta F_{\text{vdw}}$  with the corresponding energy term  $\langle U_{\text{vdw}} \rangle$ . The free energy change  $\Delta F_{\text{vdw}}$  for the addition of van der Waals solute–solvent interactions to the solute cavity is modeled by the average solute–solvent WCA attractive potential energy when the solute interacts with the solvent including the full set of Lennard–Jones interactions.

The average solute–solvent van der Waals interaction energies are calculated using explicit solvent molecular dynamics (MD) simulations carried out with the IMPACT program [29] using the OPLS [31] all-atom force field and the TIP4P [28] water model. We selected 29 conformations along the dimerization coordinate at varying separation distance  $d_i$ . Similar simulation conditions as for the FEP simulations are employed. Trajectories are collected for 500 ps and the average solute–solvent van der Waals energies are calculated by energy analysis of the saved MD trajectories.

### 3. Results and discussion

The calculated non-polar component of the solvent PMF of dimerization of alanine dipeptide is shown in Fig. 1. The solvent potential of mean force calculated in opposite directions are in close agreement, indicating that the systematic errors associated with equilibration and sampling are not significant. By averaging the forward and backward simulations we find that the free energy of dimerization is only 0.43 kcal/mol (0.6 kcal/mol for the simulation starting from the dimer state and 0.17 kcal/mol for the simulation in the reverse direction), and it slightly favors the dissociated state.

Our calculations also show that a relatively large free energy barrier exists between the associated and solvent-separated states. The height of the free energy barrier is 2.15 kcal/mol calculated from the simulation started from the solvent-separated state and 1.94 kcal/mol calculated from the simulation in the opposite direction. The PMF has a broad barrier region between 8 and 11 Å separa-

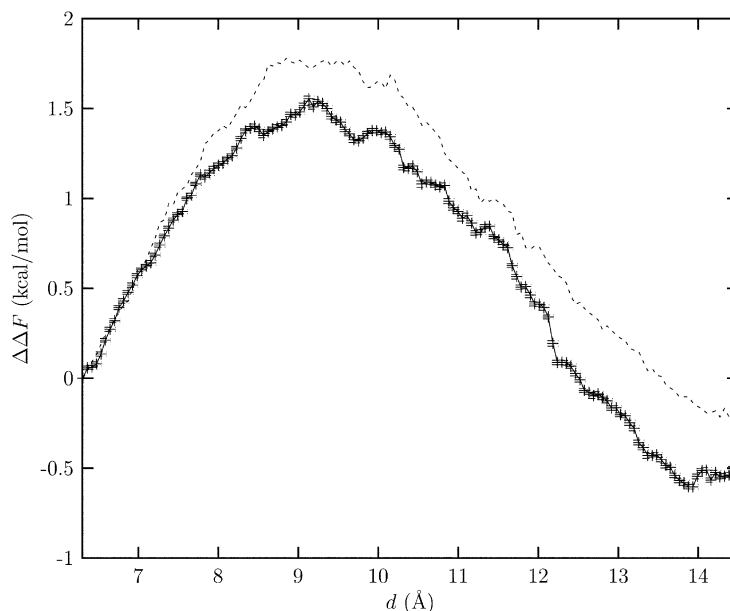


Fig. 1. The calculated non-polar component of the solvent PMF of dimerization of alanine dipeptide as a function of the  $C_{\alpha}$ – $C_{\alpha}$  distance. The line with error bars corresponds to the FEP/MD calculation starting from the dimer, the dotted line corresponds to the calculation in the opposite direction.

tion. The PMF becomes constant approximately 14 Å separation. These results are contrary to surface area models of non-polar hydration, which predict that the free energy of association should vary monotonically with the separation distance. Similar characteristics to those we have observed for the alanine dipeptide dimer have also been observed for the association of monoatomic hydrophobic solutes [15,21,25,26,32]. Studies of the thermodynamics of association of monoatomic molecules in water showed that a free energy barrier separates the contact state from the solvent-separated state. The position and magnitude of the energy barrier depends on the size of the solute molecules, temperature and pressure [15,20,33].

Fig. 2 shows representative configurations of the water molecules during the dimerization process. Our simulations do not show the occurrence of dewetted state [20,34,35], a state characterized by an empty space between two monomers larger enough to hold at least one layer of water molecules. We find that one interstitial water layer begins to form around  $d=9.25$  Å, in correspon-

dence to the barrier region of the solvent PMF indicating that, although a single layer of interstitial water molecules can exist, its formation is disfavored relative to the formation of the contact state or the fully separated state.

To examine the role of the solute–solvent van der Waals interaction energy as the basis for the non-monotonic behavior of the solvent potential of mean force of dimerization, we have computed, as described in the previous section, the average solute–solvent van der Waals energy,  $\langle U_{\text{vdw}} \rangle$ , for several conformations along the dimerization path. The results, shown in Fig. 3, clearly show that  $\langle U_{\text{vdw}} \rangle$  varies non-linearly with respect to the accessible surface area change,  $\Delta A$ . The van der Waals solute–solvent interaction energy decreases slowly when the two monomers begin to separate and then starts to decrease much faster in correspondence with the maximum of the solvent potential of mean force. We estimate the rate of change of  $\langle U_{\text{vdw}} \rangle$  in these two regimes by linear least square analysis of the data corresponding to  $\Delta A$  between 0 and 60 Å<sup>2</sup> and between 60 and 130

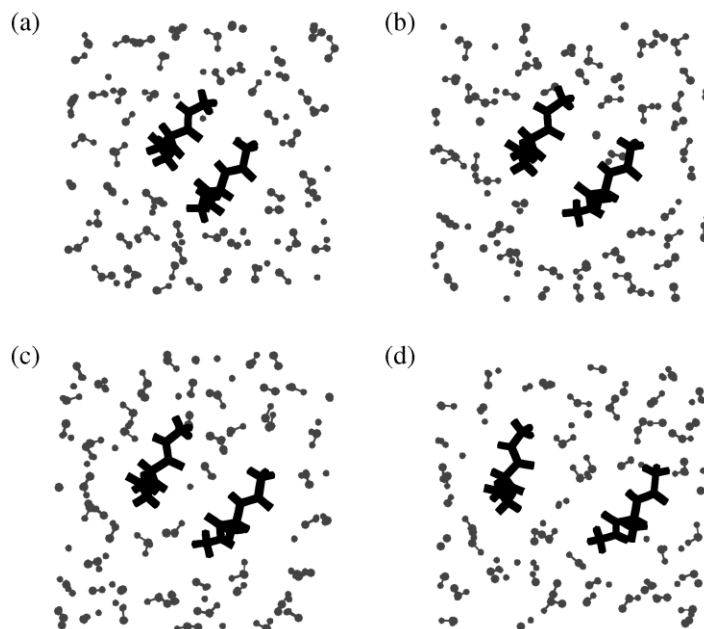


Fig. 2. Snapshots of the alanine dipeptide dimers at various separation distances  $d$  in a slice of the solvent box with dimensions  $10 \times 10 \times 5$  Å. (A)  $d = 6.3$  Å; (B)  $d = 7.5$  Å; (C)  $d = 9.3$  Å; (D)  $d = 15.3$  Å. (a) corresponds to the dimer state, (b) corresponds to the state with an empty interstitial space, (c) corresponds to the maximum in the solvent PMF (a single interstitial water layer) and (d) corresponds to the solvent-separated state.

Å<sup>2</sup>. The results of the least square analysis is represented by the two lines of different slope in Fig. 3. The rate of change of the van der Waals solute–solvent interaction energy, which is initially 33 cal/mol·Å<sup>2</sup>, abruptly changes to 82 cal/mol·Å<sup>2</sup> around  $\Delta A = 60$  Å<sup>2</sup>. This phenomenon can be interpreted in terms of the variations of hydration patterns represented in Fig. 2. At small separations the molecules do not provide enough interstitial space to allow water molecules to enter. In this regime as one monomer moves away from the other, water molecules in the second solvation shell are pushed outward. This causes a reduction of the second shell contribution to the dimer–water van der Waals interaction energy, despite the increase of the solvent accessible surface area. Nevertheless, the magnitude of the total dimer–water van der Waals interaction energy increases with increasing surface area, albeit at a small rate, due to the concomitant increase of the first solvation shell contribution to the van der Waals interaction energy, which is proportional to the surface

area. At larger separations, water molecules begin to fill the space between the two monomers. In this second regime, as the separation distance increases, both the number of water molecules in the second solvation shell increases and the average distance between solute atoms and second solvation shell water molecules decreases. Due to these combined effects the magnitude of total dimer–water van der Waals interaction energy increases with increasing surface area at a significant larger rate than in the first regime. These second solvation shell effects are not fully captured by the surface area model. The solute surface area, that measures the extent of the first solvation shell, can represent the short-range solute–solvent average interaction energy, but it cannot properly represent medium and long-range solute–solvent interactions.

The change of solute–solvent interaction energy upon dimerization is about  $-8.00$  kcal/mol. As Fig. 3 shows, the solute–solvent van der Waals energy change is much larger in magnitude than

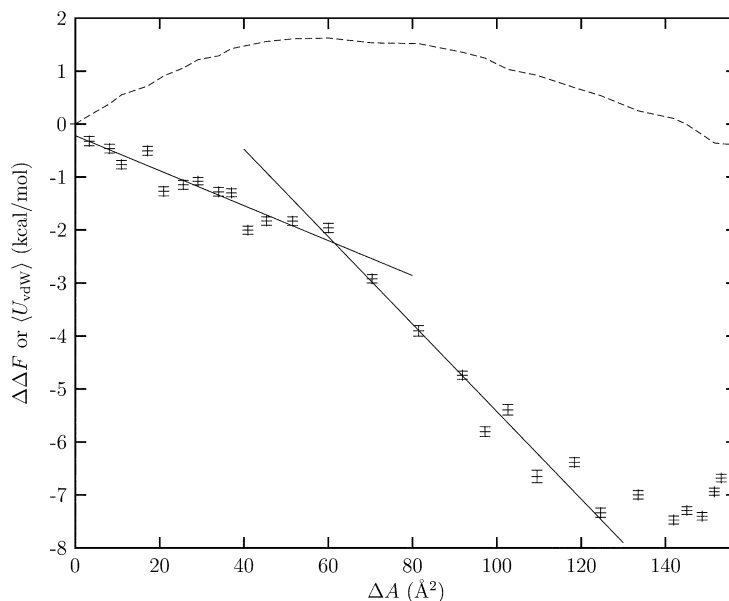


Fig. 3. Average solute–solvent van der Waals energy of the dimer as a function of the solvent accessible surface area change (points with error bars). The solid curve corresponds to the solvent PMF from Fig. 1. The two lines with different slopes are obtained by linear least square analysis of the solute–solvent van der Waals energy data for  $0 \leq \Delta A \leq 60 \text{\AA}^2$  ( $\langle U_{\text{vdW}} \rangle \approx -0.220 - 0.033 \times \Delta A$ ) and  $60 \leq \Delta A \leq 130 \text{\AA}^2$  ( $\langle U_{\text{vdW}} \rangle \approx 2.820 - 0.082 \times \Delta A$ ).

the free energy change. Clearly, the solute–solvent van der Waals energy must be matched by an almost equal but opposite cavity hydration work to yield the observed free energy profile. The cavity component of the PMF approximately corresponds to the residual,  $\Delta\Delta F - \langle U_{\text{vdW}} \rangle$ , between the PMF and the solute–solvent van der Waals interaction energy. The cavity component calculated in this way is of similar magnitude but of opposite sign to the solute–solvent van der Waals interaction energy. The cavity component is also found to vary at an approximately constant rate with respect to the surface area. We conclude, therefore, that the non-linear behavior of the solute–solvent van der Waals energy is primarily responsible for the non-monotonic dependence of the PMF with respect to the surface area. At short separation distances the solute–solvent van der Waals term varies less rapidly than the cavity term resulting in an increase of the PMF. In correspondence to the maximum of the PMF, the solute–solvent van der Waals energy begins to vary faster

than the cavity term, resulting in the decrease of the PMF.

The observed behavior of the PMF cannot be reproduced by a simple surface area model. Our analysis suggests, however, that a model based on the solute surface area and a geometrical estimator able to capture the observed behavior of the solute–solvent van der Waals interaction energy could be capable of reproducing the calculated PMF. Non-polar hydration free energy models with these characteristics have been recently proposed [11,13,27]. Here, we analyze our data with the model of Gallicchio et al. [13]:

$$\Delta\Delta F = \Delta F_{\text{cav}} + \Delta F_{\text{vdW}} = \gamma\Delta A + \alpha\Delta \left( \sum_i \frac{a_i}{(B_i + R_w)^3} \right) \quad (7)$$

where  $\Delta F_{\text{cav}}$  is modeled using the solvent accessible surface area and  $\Delta F_{\text{vdW}}$  is modeled using a

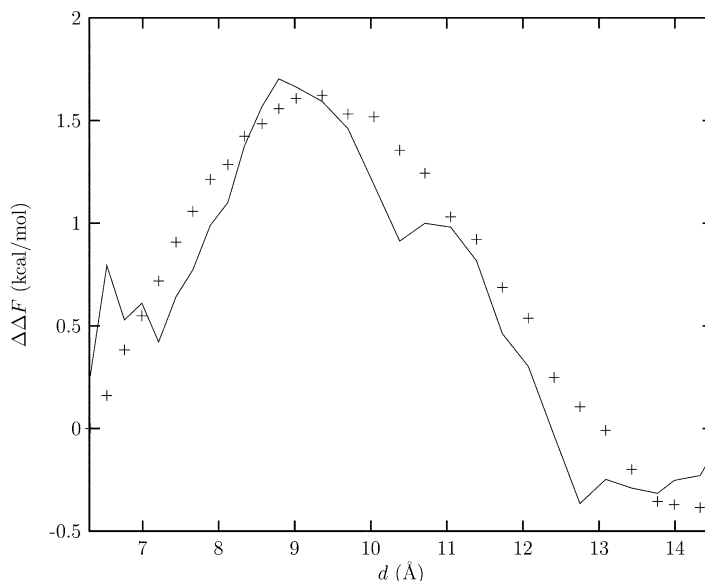


Fig. 4. The calculated (+) (from Fig. 1) and predicted (solid line) (from Eq. (7)) non-polar component of the dimerization of alanine dipeptide.

function dependent on the Born radius of each solute atom. In Eq. (7),  $\gamma$  and  $\alpha$  are adjustable parameters, and  $a_i$  is a parameter that depends on the strength of the Lennard–Jones interaction, between atom  $i$  and the solvent. It is set as

$$a_i = -\frac{16}{3}\pi\rho_w\varepsilon_{iw}\sigma_{iw}^6 \quad (8)$$

where  $\rho_w = 0.033428 \text{ \AA}^{-3}$  is the number density of water at standard conditions, and  $\varepsilon_{iw}$  and  $\sigma_{iw}$  are the OPLS force field Lennard–Jones interaction parameters for the interaction of solute atom  $i$  with the oxygen atom of the TIP4P water model. If  $\sigma_i$  and  $\varepsilon_i$  are the OPLS Lennard–Jones parameters for atom  $i$ ,

$$\sigma_{iw} = \sqrt{\sigma_i\sigma_w} \quad (9)$$

$$\varepsilon_{iw} = \sqrt{\varepsilon_i\varepsilon_w} \quad (10)$$

where  $\sigma_w = 3.15365 \text{ \AA}$  and  $\varepsilon_w = 0.155 \text{ kcal/mol}$  are the Lennard–Jones parameters of TIP4P water oxygen. In Eq. (7),  $B_i$  is the Born radius [27,36] of atom  $i$  and  $R_w = 1.577 \text{ \AA}$  is a parameter corre-

sponding to the radius of a water molecules. The Born radii are calculated by numerical integration [13].

The continuum model in Eq. (7) for the solute–solvent van der Waals interaction energy follows from integrating the  $1/r^6$  function centered on each solute atom over the solvent region assuming homogeneous solvent density, and by approximating this integral by an estimator proportional to the cube of the inverse Born radius [13]. This model is not expected to reproduce in detail the effects of molecular rearrangements of the hydration layer (see Fig. 2) that can only be resolved using an explicit representation of the solvent. It can, however, capture the essential variations of hydration geometry that are at the basis of the observed non-linear behavior of the solute–solvent van der Waals energy with respect to the accessible surface area.

The results of fitting Eq. (7) to the calculated PMF are shown in Fig. 4. The values of the parameters resulting from the fitting are  $\gamma = 0.050 \text{ cal/mol}\cdot\text{\AA}^2$  and  $\alpha = 0.95$  in reasonable agreement with the expected values of these parameters based on previous studies [13,14]. The agreement

between the calculated PMF and the predicted PMF from Eq. (7) is excellent, indicating that, with proper parameterization, this non-polar hydration free energy model [13] can accurately reproduce hydrophobic interactions of the kind represented by the alanine dipeptide dimerization studied here.

#### 4. Conclusions

We have calculated the non-polar component of the potential of mean force of dimerization of alanine dipeptide. We find that the non-polar solvation component of the free energy of dimerization is approximately zero. A relatively large free energy barrier, corresponding to the intermediate state characterized by a single layer of interstitial water molecules, separates the dimer from the solvent-separated state.

The non-monotonic behavior of the solvent PMF is rationalized in terms of the interplay between the cavity and solute–solvent van der Waals interaction energy components of the non-polar hydration free energy. These components are much larger in magnitude than the PMF and oppose each other. The cavity component is approximately proportional to the solute surface area, whereas the solute–solvent attractive interaction energy varies slowly at small separations and faster at an intermediate separation, resulting in the observed free energy barrier of the PMF. The behavior of the solute–solvent attractive interaction energy component is rationalized in terms of the variations, in two different regimes, of the medium-range solute–solvent interaction energy, which are not captured by the solute surface area. At short separation distances the number of medium-range solute–solvent interactions decreases as one monomer moves away from the other. At longer separation distances, instead, due to the concomitant formation of an interstitial hydration layer, the number of medium-range solute–solvent interactions increases as the separation of the two monomers increases.

The calculated PMF cannot be reproduced by a non-polar hydration free energy model based only on the solute surface area. We show, however, that a recently proposed non-polar hydration free energy

model [13], which takes into account independently the cavity and solute–solvent interaction free energy, can be parameterized to successfully reproduce the observed PMF.

#### Acknowledgments

This work was supported in part by National Institute of Health grant GM30580. We are grateful to Professor Ronald Levy for his support and guidance during this work and for critically reading the manuscript prior to submission.

#### References

- [1] B. Honig, A. Yang, *Adv. Prot. Chem.* 46 (1995) 27–58.
- [2] K.A. Dill, *Biochemistry* 29 (1990) 7133–7155.
- [3] J. Apostolakis, P. Ferrara, A. Calfish, *J. Chem. Phys.* 110 (1999) 2099–2108.
- [4] R.M. Levy, E. Gallicchio, *Annu. Rev. Phys. Chem.* 49 (1998) 531–567.
- [5] B. Roux, T. Simonson, *Biophys. Chem.* 78 (1999) 1.
- [6] D. Sitkoff, K.A. Sharp, B. Honig, *J. Phys. Chem.* 98 (1994) 1978–1988.
- [7] T. Simonson, A. Brünger, *J. Phys. Chem.* 98 (1994) 4683–4694.
- [8] T. Ooi, M. Oobatake, G. Nemethy, A. Sheraga, *Proc. Natl. Acad. Sci. USA* 84 (1987) 3086.
- [9] G.I. Makhatadze, P.L. Privalov, *J. Mol. Biol.* 232 (1993) 639–659.
- [10] L. Zhang, E. Gallicchio, R. Friesner, R.M. Levy, *J. Comp. Chem.* 22 (2001) 591–607.
- [11] R. Levy, L. Zhang, E. Gallicchio, A. Felts, *J. Am. Chem. Soc.* 125 (2003) 9523–9530.
- [12] A. Felts, E. Gallicchio, A. Wallqvist, R. Levy, *Proteins: Struct. Funct. Genet.* 48 (2002) 404–422.
- [13] E. Gallicchio, R.M. Levy, *J. Comput. Chem.* 2003, In Press.
- [14] E. Gallicchio, M.M. Kubo, R.M. Levy, *J. Phys. Chem. B* 104 (2000) 6271–6285.
- [15] J. Pitarch, V. Moliner, J. Pascual-Ahuir, A. Silla, I. Tuñón, *J. Phys. Chem.* 100 (1996) 9955–9959.
- [16] J.W. Pitera, W.F. van Gunsteren, *J. Am. Chem. Soc.* 123 (2001) 3163–3164.
- [17] H.S. Ashbaugh, E.W. Kaler, M.E. Paulaitis, *Biophys. J.* 75 (1998) 755–768.
- [18] H.S. Ashbaugh, E.W. Kaler, M.E. Paulaitis, *J. Am. Chem. Soc.* 121 (1999) 9243–9244.
- [19] R.M. Jackson, J.E. Sternberg, *J. Mol. Biol.* 250 (1995) 258–275.
- [20] A. Wallqvist, B.J. Berne, *J. Phys. Chem.* 99 (1995) 2893–2899.

- [21] W.L. Jorgensen, J.K. Buckner, S. Boudon, J. Tirado-Rives, *J. Chem. Phys.* 89 (1988) 3742.
- [22] L.R. Pratt, D. Chandler, *J. Chem. Phys.* 67 (1977) 3683–3704.
- [23] L.R. Pratt, G. Hummer, A. Garcia, *Biophys. Chem.* 51 (1994) 147–160.
- [24] C. Pangali, M. Rao, B.J. Berne, *J. Chem. Phys.* 71 (1979) 2975–2981.
- [25] D. Belle, S. Wodak, *J. Am. Chem. Soc.* 115 (1993) 647–652.
- [26] M.H. New, B.J. Berne, *J. Am. Chem. Soc.* 117 (1995) 7172–7179.
- [27] E. Gallicchio, L. Zhang, R. Levy, *J. Comp. Chem.* 23 (2002) 517–529.
- [28] W.L. Jorgensen, J. Chandrasekhar, J.D. Madura, R.W. Impey, M.L. Klein, *J. Chem. Phys.* 79 (1983) 926.
- [29] D.B. Kitchen, F. Hirata, J.D. Westbrook, R.M. Levy, D. Kofke, M. Yarmush, *J. Comput. Chem.* 11 (1990) 1169.
- [30] J.D. Weeks, D. Chandler, H.C. Andersen, *J. Chem. Phys.* 54 (1971) 5237–5247.
- [31] W.L. Jorgenson, D.S. Maxwell, J. Tirado-Rives, *J. Am. Chem. Soc.* 118 (1996) 11 225–11 235.
- [32] K. Watanabe, H.C. Andersen, *J. Phys. Chem.* 90 (1986) 795.
- [33] V. Payne, N. Matubayasi, L. Murphy, R. Levy, *J. Phys. Chem. B* 101 (1997) 2054–2060.
- [34] K. Lum, D. Chandler, J. Weeks, *J. Phys. Chem. B* 103 (1999) 4570–4577.
- [35] A. Wallqvist, E. Gallicchio, R.M. Levy, *J. Phys. Chem. B* 105 (2001) 6745–6753.
- [36] D. Qiu, P.S. Shenkin, F.P. Hollinger, C.W. Still, *J. Phys. Chem. A* 101 (1997) 3005–3014.